analytical chemistry

Article

Cite This: Anal. Chem. 2018, 90, 3341−3348

pubs.acs.org/ac

Investigation of Ion−Solvent Interactions in Nonaqueous Electrolytes Using in Situ Liquid SIMS

Yanyan Zhang,[†,‡,§] Mao Su,[§,∥,⊥] Xiaofei Yu,[‡,#] Yufan Zhou,[‡,#] Jungang Wang,[‡] Ruiguo Cao,[¶] Wu Xu,[¶] Chongmin Wang,[‡] Donald R. Baer,[‡] Oleg Borodin,[□] Kang Xu,[□] Yanting Wang,[§,⊥] Xue-Lin Wang,[#] Zhijie Xu,*[,∥] Fuyi Wang,*[,†,§] and Zihua Zhu*[,‡]

[†]Beijing National Laboratory for Molecular Sciences, National Centre for Mass Spectrometry in Beijing, CAS Key Laboratory of Analytical Chemistry for Living Biosystems, Institute of Chemistry, Chinese Academy of Sciences, Beijing 100190, P. R. China

[‡]Environmental Molecular Sciences Laboratory, [∥]Computational Mathematics Group, Physical and Computational Sciences Directorate, and [¶]Energy Processes and Materials Division, Energy and Environmental Directorate, Pacific Northwest National Laboratory, Richland, Washington 99354, United States

[§]University of Chinese Academy of Sciences, Beijing 100049, P. R. China

[⊥]CAS Key Laboratory of Theoretical Physics, Institute of Theoretical Physics, Chinese Academy of Sciences, 55 East Zhongguancun Road, P.O. Box 2735, Beijing 100190, P. R. China

[#]School of Physics, State Key Laboratory of Crystal Materials and Key Laboratory of Particle Physics and Particle Irradiation (MOE), Shandong University, Jinan, 250100, P. R. China

[□]Electrochemistry Branch, Power and Energy Division, Sensor and Electron Devices Directorate, U.S. Army Research Laboratory, Adelphi, Maryland 20783, United States

Supporting Information

ABSTRACT: Ion−solvent interactions in nonaqueous electrolytes are of fundamental interest and practical importance, yet debates regarding ion preferential solvation and coordination numbers persist. In this work, in situ liquid SIMS was used to examine ion−solvent interactions in three representative electrolytes, i.e., lithium hexafluorophosphate ($LiPF_6$) at 1.0 M in ethylene carbonate (EC)−dimethyl carbonate (DMC) and lithium bis(fluorosulfonyl)imide (LiFSI) at both low (1.0 M) and high (4.0 M) concentrations in 1,2-dimethoxyethane (DME). In the positive ion mode, solid molecular evidence strongly supports the preferential solvation of Li^+ by EC. Besides, from the negative spectra, we also found that PF_6^- forms association with EC, which has been neglected by previous studies due to the relatively weak interaction. In both LiFSI in DME electrolytes, however, no evidence shows that FSI^- is associated with DME. Furthermore, strong salt ion cluster signals were observed in the 1.0 M $LiPF_6$ in EC−DMC electrolyte, suggesting that a significant amount of Li^+ ions stay in the vicinity of anions. In sharp comparison, weak ion cluster signals were detected in dilute LiFSI in DME electrolyte, suggesting most ions are well separated, in agreement with our molecular dynamics simulation results. These findings indicate that with virtues of little bias on detecting positive and negative ions and the capability of directly analyzing concentrated electrolytes, in situ liquid SIMS is a powerful tool that can provide key evidence for improved understanding on the ion−solvent interactions in nonaqueous electrolytes. Therefore, we anticipate wide applications of in situ liquid SIMS on investigations of various ion−solvent interactions in the near future.

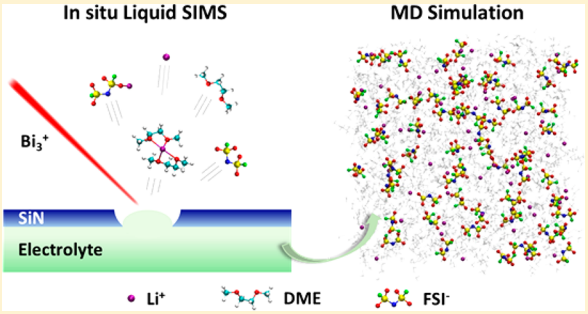

Lithium (Li) ion batteries are the most popular power source for mobile electronic devices. More importantly, their applications in electric vehicles and energy storage have been gaining momentum in the past decade. However, since their initial development, the mechanisms behind their chemistry remain little understood. For example, Li^+ solvation sheath structure has been a topic of debate for more than 10 years. This topic is of great importance not only due to the fact that the Li^+ solvation sheath affects Li^+ transport in the bulk electrolyte but also because it exerts a significant effect on the chemistry of solid−electrolyte interphase (SEI) formation and the kinetics of Li^+ desolvation at the formed SEI.[1−5]

Extensive efforts, with both experimental techniques such as resonance infrared (IR) spectroscopy,[6−8] nuclear magnetic resonance (NMR),[3,9,10] Raman,[11−13] and near ambient pressure photoemission (NAPP)[14] and computational ap-

Received: November 27, 2017
Accepted: February 6, 2018
Published: February 6, 2018

DOI: 10.1021/acs.analchem.7b04921
Anal. Chem. 2018, 90, 3341−3348

proaches including density functional theory (DFT)[7,15−21] and force field-based molecular dynamics (MD),[22] have been made to investigate the interaction of Li^+ with electrolyte solvents. However, many key questions remain debatable, especially among computational efforts. For example, although it has been widely accepted that Li^+ is well solvated in electrolytes, its coordination number, i.e., how many solvent molecules a Li^+ can accommodate in its primary solvation sheath, is still being debated. Taking the electrolyte of lithium bis(fluorosulfonyl)-imide (LiFSI) in 1,2-dimethoxyethane (DME) as an example, one DFT study showed that the coordination number of DME to a Li^+ is two as the binding energy of Li^+ with three or more DME molecules is greater than zero,[23] but other MD simulations indicated that at low salt concentrations most Li^+ were coordinated by three DME in accord with the crystal structure, with the Li^+ solvation number decreasing with increasing salt concentration.[24,25] In addition, whether Li^+ prefers any solvent molecules in mixed carbonate solvents also remains controversial. In most widely used electrolyte formulations, lithium hexafluorophosphate ($LiPF_6$) in ethylene carbonate (EC)−dimethyl carbonate (DMC) mixture, NMR results[3,9] and a recent DFT-based Born−Oppenheimer molecular dynamics (BOMD) simulation[16] suggested that Li^+ prefers to be solvated by EC; however, another MD simulation showed a slight preference of Li^+ for DMC.[22] Another interesting question is whether Li^+ ions prefer to be fully solvated by solvent molecules or can they form ion clusters with anions in the commonly used dilute electrolytes.

Computational investigation of Li^+ solvation generally starts from quantum calculation of simple structures, e.g., a Li^+ with one or more solvent molecules/anions.[7,15−25] For example, force-field-based MD simulations generally required the quantum calculations to determine the parameters of the force field.[22] However, the quantum calculation results are hard to be verified by experimental methods, which may further influence the reliability of MD simulations.

The above-mentioned experimental techniques, such as IR, NMR, Raman, and NAPP, share a common limitation in that they only provide "chemical shift" information, i.e., the change of chemical environment of the solvent molecules, and no direct molecular information is available. Besides, they are analytical techniques for bulk solutions and cannot be used to test the structure and stability of small molecular clusters. Recently, electrospray ionization mass spectrometry (ESI-MS) was carried out to help clarify the conflicts over this critically important topic.[26,27] The major advantage of the mass spectrometric techniques is that the detection of molecular ions provides direct molecular information on Li^+−solvent complexes, which provides a more straightforward method of testing the structure and stability of the initial quantum calculation results. Using ESI-MS, Xu et al. successfully identified the composition of Li^+ solvation species as well as the coordination numbers in the solvation shell, providing very solid evidence for the preference of cyclic over acyclic carbonate molecules by Li^+,[27] which is in agreement with the stabilities of Li^+ solvates found in recent quantum chemistry calculations.[16] Thereafter, ESI-MS has become increasingly used in electrolyte research.[28−32]

Although ESI-MS has provided new and important insights, there are several intrinsic challenges still remaining. First, as most electrolytes used in Li ion batteries are sensitive to moisture,[5] instrumental modifications are required.[27] Second, ESI-MS can only work with dilute solutions, and severe challenges arise from the high viscosity of concentrated electrolytes, which prevents the successful formation of electrolyte microbeads through the spraying nozzle. This disadvantage restricts its application in the study of a class of electrolytes that are gaining increasing interest due to their unusual properties and potential in the next-generation high-capacity rechargeable Li batteries.[25,33,34]

Recently, in situ liquid secondary ion mass spectrometry (SIMS) was developed, allowing us to directly analyze liquid and liquid interfaces to obtain molecular information.[35−39] The principle is schematically shown in Figure 1a. The in situ liquid

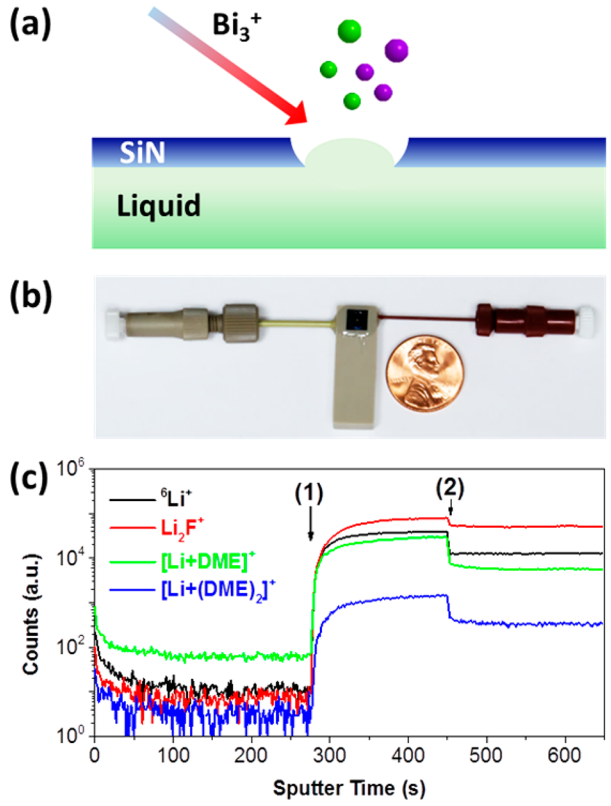

Figure 1. (a) Schematic illustration of in situ liquid SIMS measurement. The cell was presealed, and a thin silicon nitride (SiN) membrane was used to separate the liquid electrolyte in the cell from the outside vacuum. During in situ SIMS analysis, a fine-focused primary ion beam is used to drill a small aperture (~2 μm in diameter) through the SiN membrane, and then mass spectra of the sealed liquid was collected. (b) Photograph of the assembly of the vacuum compatible liquid cell. (c) SIMS depth profiles of 4.0 M LiFSI in DME electrolyte in the positive ion mode. Arrow (1) points to the time when the SiN membrane was punched through exposing the liquid electrolyte within the cell. Arrow (2) refers to the time when the Bi_3^+ pulse width was reduced from 150 to 50 ns for a better mass resolution.

SIMS approach adds new and important versatility to the investigation of ion−solvent interactions. First, no instrumental modification is needed, as the novelty of the technique resides in the microfluidic cell design (Figure 1b), which can be used in any commercial SIMS instrument. Second, analysis of concentrated electrolytes is feasible using in situ liquid SIMS, as no spraying is required. Most importantly, in situ liquid SIMS can be used to examine formation and dynamic change of electric double layer at electrode−electrolyte interfaces.[39]

DOI: 10.1021/acs.analchem.7b04921
Anal. Chem. 2018, 90, 3341−3348

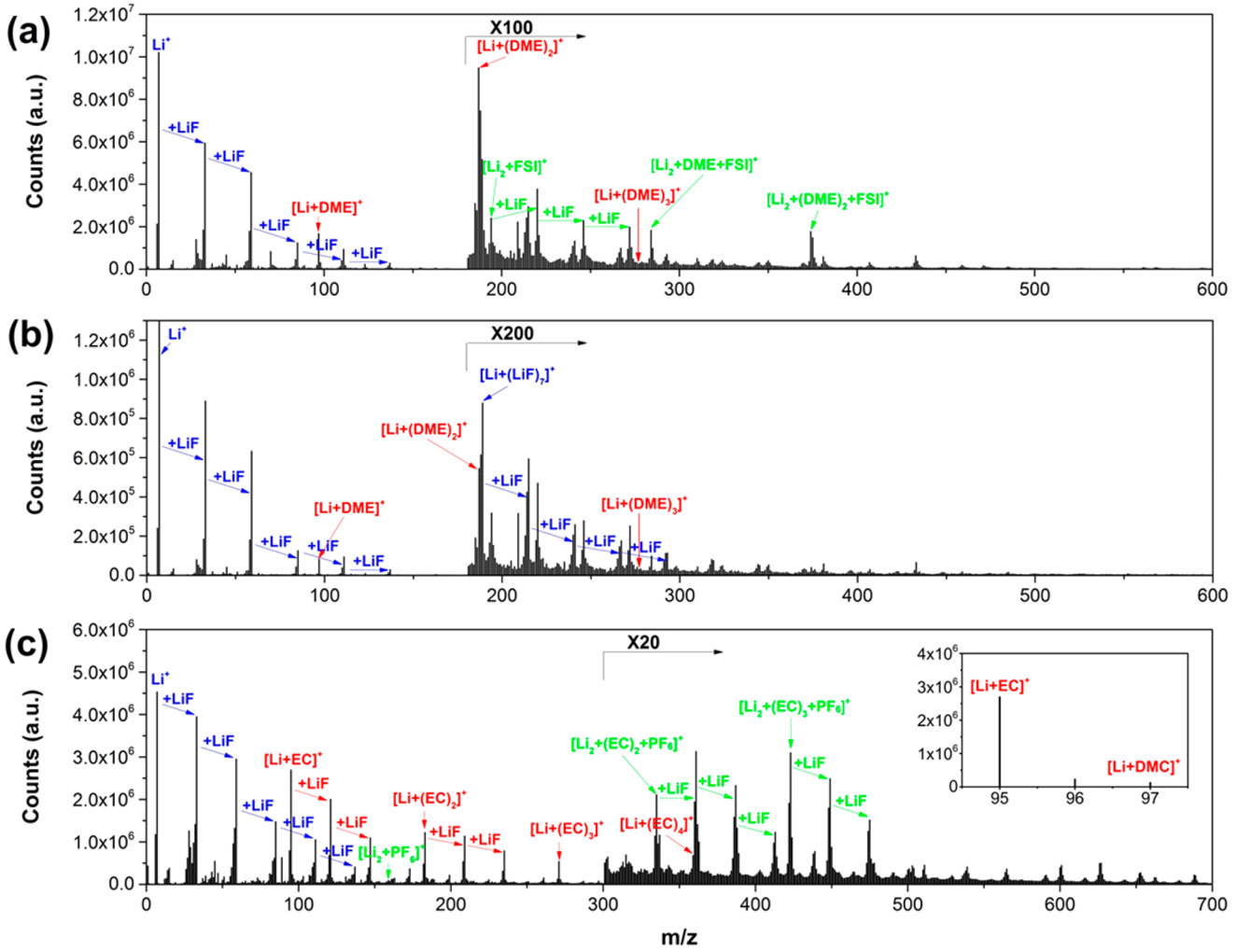

Figure 2. Positive ion spectra of (a) 1.0 M LiFSI in DME electrolyte, (b) 4.0 M LiFSI in DME electrolyte, and (c) 1.0 M $LiPF_6$ in EC−DMC electrolyte. Inset: enlarged $[Li + EC]^+$ and $[Li + DMC]^+$ regions of the spectra for the $LiPF_6$ in EC−DMC electrolyte. Data collection time for each spectrum is ∼200 s.

In this work, we used three model electrolyte systems to demonstrate the unique advantages of in situ liquid SIMS in investigating ion−solvent molecular interactions, including $LiPF_6$ at 1.0 M in EC−DMC (1:2 v/v) and LiFSI at both low (1.0 M) and high (4.0 M) concentrations in DME. $LiPF_6$ in EC−DMC has been the most typical formulation in current Li ion batteries, but the preferential solvation of Li^+ ion in mixed solvents of EC and DMC is still in debate. The 4.0 M LiFSI in DME electrolyte became a very promising candidate for the next generation Li−metal batteries.[25] All these three electrolytes are successfully analyzed in this work with in situ liquid SIMS. The obtained results provide very solid molecular evidence of the preferential solvation of Li^+ by EC and, more interestingly, the formed association of PF_6^- with EC which has been neglected by previous studies. Moreover, we combined the in situ liquid SIMS technique with MD simulation to examine the coordination number of a Li^+ ion in its solvation sheath and ion clusters in the electrolytes, which aid in better understanding ion−solvent interactions in these nonaqueous electrolytes.

EXPERIMENTAL SECTION

Preparation of Electrolytes. $LiPF_6$ (molecular weight (MW) = 152), DME ($C_4H_{10}O_2$, MW = 90), EC ($C_3H_4O_3$, MW = 88), and DMC ($C_3H_6O_3$, MW = 90) of battery grade were purchased from BASF Battery Materials, and LiFSI ($LiF_2NS_2O_4$, molecular weight (MW) = 187) of battery grade was supplied by Nippon Shokubai Co., Ltd. All chemicals were used as received. Electrolyte solutions comprised of 1.0 or 4.0 M LiFSI in DME and 1.0 M $LiPF_6$ in EC−DMC (1:2 v/v) were prepared in an argon-filled MBraun glovebox.

Fabrication of the Vacuum Compatible Liquid Cell. The liquid cell was fabricated on a polyether ether ketone (PEEK) block using the method reported in our previous publication with some adaptations.[36] In brief, a liquid chamber with a size of 3.0 mm (L) × 3.0 mm (W) × 0.3 mm (H) was machined on the PEEK block with two liquid channels for the introduction of electrolytes. The silicon frame (5.0 mm (L) × 5.0 mm (W) × 0.2 mm (H)) with a 100 nm thick silicon nitride (SiN) membrane immobilized beneath it was placed on top of the liquid chamber and sealed by epoxy glue. Following the assembly of the cell, the investigated electrolyte could be introduced into the liquid chamber in an argon-filled glovebox. After the ends of two liquid channels were sealed, the liquid cell was loaded on a ToF-SIMS sample holder and then introduced into the main chamber of the ToF-SIMS instrument for in situ liquid SIMS analysis. A photograph of the liquid cell is shown in Figure 1b.

DOI: 10.1021/acs.analchem.7b04921
Anal. Chem. 2018, 90, 3341−3348

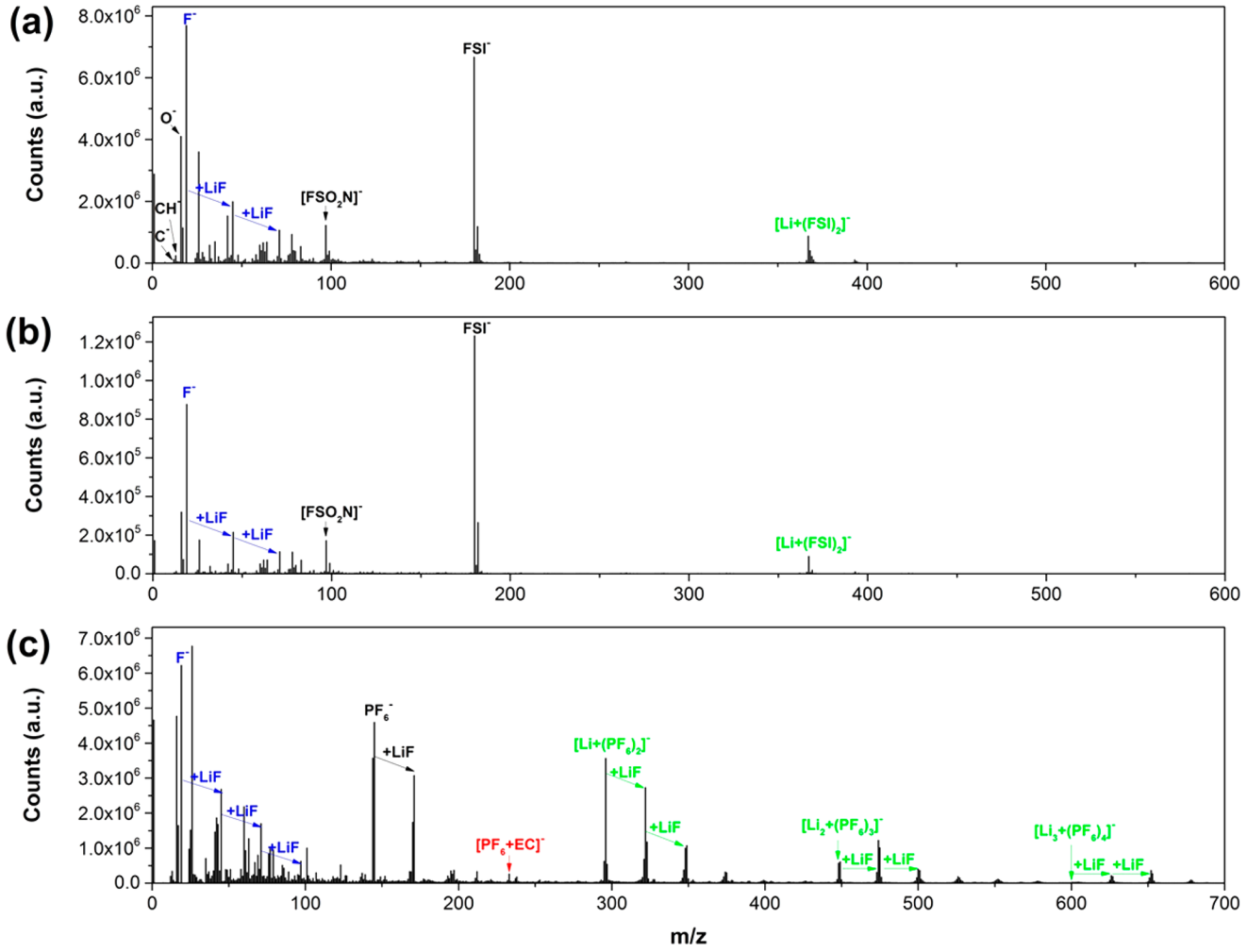

Figure 3. Negative ion spectra of (a) 1.0 M LiFSI in DME electrolyte, (b) 4.0 M LiFSI in DME electrolyte, and (c) 1.0 M $LiPF_6$ in EC−DMC electrolyte. Data collection time for each spectrum is ∼200 s.

In Situ Liquid SIMS Measurement. The ToF-SIMS measurements were conducted using a ToF-SIMS 5 instrument (ION-TOF GmbH, Münster, Germany). The primary ion beam consists of pulsed 25 keV Bi_3^+ with a 10 kHz repeating rate, which was focused to ∼500 nm in diameter. The pulse width was about 150 ns, and the corresponding beam current was ∼0.36 pA. For each measurement, the beam was scanned on a round area of ∼2 μm in diameter around the center of the SiN window, and an aperture was drilled. The penetration of the SiN membrane was indicated by a sharp increase in signal intensity of the species in electrolytes within the liquid chamber of the cell (e.g., at ∼270 s in Figure 1c). When signals became relatively stable (e.g., at ∼450 s in Figure 1c), the Bi_3^+ pulse width was changed from 150 to 50 ns for a better mass resolution. After a spectrum with reasonable signal intensities was collected (e.g., ∼ 200 s), the measurement could be stopped. Mass spectra reflecting liquid information were reconstructed from the time when the pulse width was changed to 50 ns as pointed by the arrow (2) on the obtained depth profiles in Figure 1c. The vacuum pressure in the main chamber was $1-2 \times 10^{-6}$ mbar during measurement. More details of the instrumental settings of in situ liquid SIMS measurement can be found in our recent publication.[40] On each SiN membrane, 2−3 apertures could be drilled safely during SIMS analysis. If more apertures were drilled, a SiN membrane might break, and such a failure might lead to some damage to the instrument.

MD Simulation. MD simulations of 1.0 M LiFSI in DME electrolytes were performed at the temperature T = 333 K. The simulation box is 4.9 × 4.9 × 4.9 nm^3 with 576 DME molecules, 64 Li^+, and 64 FSI^- ions inside. The simulations were run for 15 ns in the NVT ensemble to collect data. A many-body polarizable force field APPLE&P was used.[41] A Li^+ is considered coordinated if the distance between the Li^+ and oxygen atoms in DME or FSI^- is shorter than 0.35 nm, which corresponds to the first valley of the Li−O radial distribution function.

RESULTS AND DISCUSSION

Data Repeatability. Reasonable data repeatability of in situ liquid SIMS measurement has been described in our previous publications.[37,38,42] Figure S-1 shows negative ion spectra of $LiPF_6$ in EC−DMC collected with five individual microfluidic cells on four different days over a period of eight months. Essentially identical data sets further confirm good repeatability of in situ liquid SIMS measurement.

Analysis of Dilute and Concentrated LiFSI in DME Electrolytes. Unlike with ESI-MS, analysis of concentrated electrolyte is feasible using liquid SIMS. Figures 2a and 2b show the positive ion spectra of the dilute (1.0 M) and concentrated

DOI: 10.1021/acs.analchem.7b04921
Anal. Chem. 2018, 90, 3341−3348

(4.0 M) LiFSI in DME electrolytes. The two spectra look similar to a series of $[Li_{n+1}F_n]^+$ peaks, which may come from damaged LiFSI species at the sputtering interface. Besides, the solvated Li ion peaks, e.g., $[Li + DME]^+$ (m/z = 97) and $[Li + (DME)_2]^+$ (m/z = 187) were observed. The relative intensities of the solvated Li ion peaks (versus $[Li_{n+1}F_n]^+$) in the spectrum of the dilute electrolyte are higher than those in the concentrated electrolyte. This is easy to understand because the ratio of solvent molecules versus Li^+ ions is much higher in the dilute electrolyte and most Li^+ ions can be fully solvated and well-separated from FSI^- ions. Such a situation benefits formation of more $[Li + DME]^+$ but less $[Li_{n+1}F_n]^+$ during SIMS analysis.

Figures 3a and 3b depict the negative ion spectra of the dilute (1.0 M) and the concentrated (4.0 M) LiFSI in DME electrolytes. The two negative spectra also resemble each other with F^- and FSI^- dominating both spectra. The relative intensity of C^-, CH^-, and O^- versus F^- in the spectrum of the dilute electrolyte is higher than that in the concentrated electrolyte, which is in agreement with higher populations of solvent molecules in the dilute electrolyte. In addition, no solvated negative ions were observed, indicating the weak solvation of anions.

The most significant difference between the spectra of the dilute and concentrated electrolyte in the positive or negative ion mode is signal intensity. We found that the signal intensity from the dilute electrolyte in the negative spectra (Figure 3a) is almost 1 order of magnitude higher than that from the concentrated electrolyte (Figure 3b), which is also observed in the positive ion mode (Figures 2a and 2b). A possible explanation is that the fluidity of the concentrated electrolyte is much lower than that of the dilute electrolyte, leading to the accumulation of more damaged materials at the sputtering interface.

Preferential Solvation of Li^+ Ion in Mixed Solvents. $LiPF_6$ (1.0 M) in EC−DMC electrolyte represents the most typical formulation in Li ion batteries. NMR,[3,9] ESI-MS,[27] and DFT calculations[16] show that Li^+ ions prefer to be solvated by EC. While previous MD simulation[22] suggested that DMC is slightly more favored over EC for Li^+ solvation, BOMD simulations[16] and our MD simulations using revised APPLE&P force field[30] indicate a preference for the Li^+ to be solvated by EC. The in situ liquid SIMS data strongly support the "EC-preference" school. From the positive spectrum of the 1.0 M $LiPF_6$ in EC−DMC electrolyte (Figures 2c and S-2), signal intensities of EC-containing species, such as $[Li + EC]^+$ (m/z = 95), $[Li + (EC)_2]^+$ (m/z = 183), and $[Li + (EC)_3]^+$ (m/z = 271), are almost 2 orders of magnitude stronger than those of respective DMC-containing species, i.e., $[Li + DMC]^+$ (m/z = 97), $[Li + EC + DMC]^+$ (m/z = 185), and $[Li + (EC)_2 + DMC]^+$ (m/z = 273), indicating an absolute dominance of Li^+ solvation by EC. Taking into account a slightly higher reduction potential of the $[Li + EC]^+$ vs $[Li + DMC(cis-cis)]^+$ complexes as predicted from DFT calculations,[43] the preference of the Li^+ cation to be coordinated by EC explains why SEI is expected to be originated from reductive decomposition products from EC rather than DMC.

As multicomponent electrolytes could lead to significant improvements in battery performances, where preferential solvation was hypothesized to play a critical role,[29,44,45] we expect a promising application of in situ liquid SIMS in offering direct molecular insights in this increasingly interesting field.

Examination of Coordination Number. The debate over coordination number of Li^+ in nonaqueous electrolytes has been continuing for more than a decade. Herein, our MD simulation suggests that most Li^+ ions in 1.0 M LiFSI in DME are fully solvated with three DME molecules (see Figures 4 and S-3). However, DFT calculation based on the Polarizable Continuum Model (PCM) shows that $[Li + (DME)_{1-2}]^+$ ions instead of $[Li + (DME)_3]^+$ are stable, and $[Li + DME]^+$ is more stable than $[Li + (DME)_2]^+$.[23] Interpretation of such calculations is difficult, however, because they inherently depend on ability of the PCM model to reproduce Li^+ solvation rather than predicting the Li^+ coordination number.

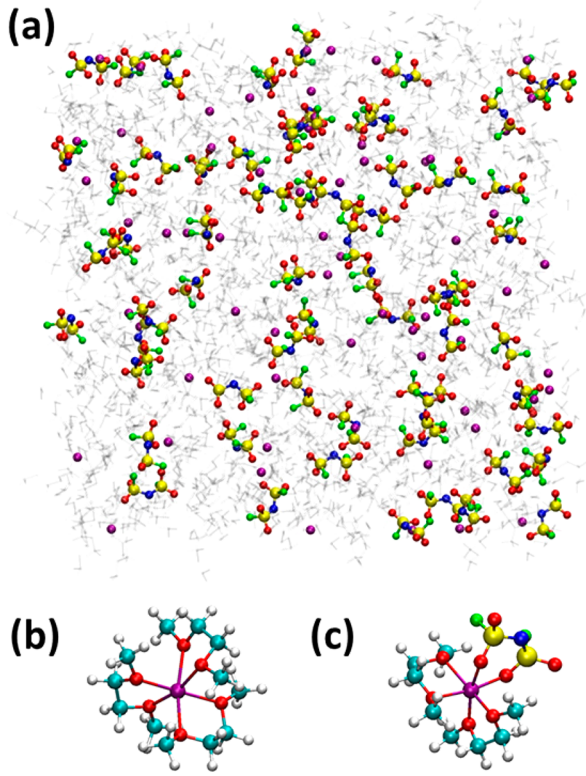

Figure 4. Molecular dynamics (MD) simulation of 1.0 M LiFSI in DME. (a) Snapshot of the bulk electrolyte. The ions are presented as colored balls (Li, purple; O, red; N, blue; S, yellow; F, green), and solvent molecules are shown as gray rods for better clarity. (b) Structure of fully solvated Li^+ ions with three DME molecules. (c) Typical ion cluster observed in 1.0 M LiFSI in DME. In (b) and (c), the DME solvent molecules are also shown as colored balls (C, cyan; H, gray; O, red).

In this work, data obtained by in situ liquid SIMS (Figures 2a and 2b) have the $[Li + DME]^+$ signal clearly observed, with the $[Li + (DME)_2]^+$ signal observable but relatively weak, and the $[Li + (DME)_3]^+$ signal too weak to be detected. These results indicate that binding of the third DME to Li^+ in gas phase is much weaker than that for the first two DME.

Quantum chemistry calculations and MD simulation suggest that $[Li + (EC)_{1-4}]^+$ are all stable in vacuum, and $[Li + (EC)_4]^+$ is the most stable one.[16,22] This is only in partial agreement with our SIMS data. Figure 2c shows that all $[Li + (EC)_{1-3}]^+$ signals are strong, but $[Li + (EC)_4]^+$ is very weak. A comparison of signal intensity (after correction of signal saturation) of $[Li + (EC)_n]^+$ ions is shown in Figure S-4. The intensity of the $[Li + (EC)_2]^+$ is slightly weaker than that of the

DOI: 10.1021/acs.analchem.7b04921
Anal. Chem. 2018, 90, 3341−3348

$[Li + EC]^+$, and about eight times that of the $[Li + (EC)_3]^+$. However, the signal intensity of $[Li + (EC)_4]^+$ is much weaker (almost 2 orders of magnitude) than that of $[Li+ (EC)_3]^+$, indicating a much worse stability of $[Li + (EC)_4]^+$ than $[Li + (EC)_{1-3}]^+$. Similar with the previous ESI-MS data,[27] this work also designates $[Li + (EC)_4]^+$ as the least likely species. This trend is consistent with the progressively smaller reaction energy for $[Li + (EC)_n]^+ + EC \rightarrow [Li + (EC)_{n+1}]^+$ with increasing n observed in DFT calculations.[22,46]

It should be mentioned that each DME molecule has two oxygen atoms that can coordinate with a Li^+, while each EC molecule has only one oxygen atom to coordinate with a Li^+. Our above data suggest that the first two coordination interactions are very strong, the third one becomes much weaker, the fourth one may be only marginally energetically favorable, and further coordination interactions may become energetically more unfavorable. Some of the previous modeling results showed that the coordination number of EC to Li^+ can be as high as six,[47] which does not agree with our results or the results of IR[7] or Raman[11,13] experiments, BOMD simulations,[16,17] or X-ray absorption spectroscopy.[48]

Solvation of Anions. Limited understanding has been reported toward anion−solvent interactions in nonaqueous electrolytes. One of the reasons is that solvation of salt anions in Li ion battery electrolytes is generally believed to be weak, at least much weaker than solvation of Li^+ ions,[1] because anions are significantly larger than naked Li^+ ions. A more important reason may be that the traditional bulk analysis methods cannot distinguish weak solvation of anions from strong solvation of Li^+ ions.

The negative ion spectrum of 1.0 M $LiPF_6$ in EC−DMC electrolyte depicted in Figure 3c shows a clear solvated anion peak $[PF_6 + EC]^-$ (m/z = 233), strongly suggesting that PF_6^- can also be solvated by EC molecules in EC−DMC solvent mixture, although its low intensity indicates that such association may be weak and nonpervasive throughout the solution. Similar to solvated Li^+ ions, $[PF_6 + DMC]^-$ (m/z = 235) was weaker (as shown in Figure S-5), suggesting that preferential solvation also occurs for anions. The above observation further supports that easier polarization of EC than DMC plays a key role for preferential solvation. Moreover, it also serves as a strong statement that in situ liquid SIMS is a much more sensitive tool than ESI-MS in detecting minor but important species, particularly negative ions. On the other hand, $[FSI + DME]^-$ ion was not observed in either dilute or concentrated electrolytes (Figures 3a and 3b), implying that FSI^- is a much more liberated anion without solvation sheath drag. This observation may be attributed to relatively large size of FSI^- and low polarization of DME molecules, as well as to the fact that HFSI is a stronger superacid than HPF_6. We believe that solvation of anions may necessarily be considered in certain cases, despite the fact that it is indeed much weaker than the solvation of Li^+ ions.

Ion Clusters in Dilute Electrolyte. Computer simulation results suggest that small salt ion clusters, e.g., Li^++FSI^-, exist in the electrolyte even in dilute (1.0 M) situation. Examples of the distribution/population of the ion clusters extracted from a snapshot are shown in Figure S-3. In negative ion spectra, ion clusters can be observed (Figure 3). An interesting observation is that the signals for $[Li_n + (FSI)_{n+1}]^-$ cluster ions are weak, even in the 4.0 M concentrated electrolyte (Figures 3a and 3b), while the signals for $[Li_n + (PF_6)_{n+1}]^-$ (and $[Li_n + (PF_6)_{n+1} + (LiF)_{1-3}]^-$) cluster ions in the $LiPF_6$ in EC−DMC electrolyte are much stronger (Figure 3c). A previous MD simulation suggested that most ions form clusters in the concentrated LiFSI in DME electrolyte.[25] This study suggests that the $[Li_n + (FSI)_{n+1}]^-$ ions may not be stable under vacuum condition. As a comparison, $[Li_n + (PF_6)_{n+1}]^-$ cluster ion signals are strong, suggesting $[Li_n + (PF_6)_{n+1}]^-$ ion clusters are relatively stable in vacuum. Therefore, it is reasonable to expect that most ions prefer to be isolated from each other in the 1.0 M LiFSI in DME electrolyte, while more ion clusters exist in 1.0 M $LiPF_6$ in EC−DMC electrolyte. Our MD simulation results reveal most Li^+ ions (~76% on average) are fully solvated in 1.0 M LiFSI in DME electrolyte (Figure S-3), consistent with SIMS data.

What's interesting is that the solvated positive cluster ions, such as $[Li_2 + DME + FSI]^+$ (m/z = 284), $[Li_2 + (DME)_2 + FSI]^+$ (m/z = 374), $[Li_2 + (EC)_2 + PF_6]^+$ (m/z = 335), and $[Li_2 + (EC)_3 + PF_6]^+$ (m/z = 423), are obvious, while solvated negative cluster ions are too weak to be detected. A comparison of signal intensities of $[Li_2 + PF_6 + (EC)_n]^+$ ions normalized to $[Li_2 + PF_6]^+$ ion intensity and those of $[Li+(PF_6)_2 + (EC)_n]^-$ ions normalized to $[Li + (PF_6)_2]^-$ ion intensity detected in the 1.0 M $LiPF_6$ in EC−DMC electrolyte system was shown in Figure S-6. This phenomenon further supports that Li^+ ions are much easier to be solvated than anions.

Recombination Effect. Damage-recombination is a common issue in SIMS analysis. Because ion bombardment introduces significant perturbation at the sample surface, some chemical bonds break, and the debris can recombine at sample surface to form some new species that do not exist in the original sample.[49−53] It should be noted that most recombination occurs at the sputter interface, and very little occurs in the plume (i.e., gas phase) due to the low collisional probability in the plume.[50−52] In our research, $[Li_{n+1}F_n]^+$ and $[Li_nF_{n+1}]^-$ ions come from such a damage-recombination process. However, we believe damage-recombination effect does not affect our conclusions. First, liquid samples, but not solid samples, were used in this research. Ion and solvent diffusion and recombination always quickly occur without any ion bombardment. Ion bombardment only provides some extra energy to make this process quicker with very limited effect on the final results. More importantly, we have some solid evidence to show the fragmentation effect in SIMS analysis is weaker for liquid samples than that for traditional solid samples.[54] In addition, it has been well-accepted that although quite a few ions may come from recombination, there are a significant amount of molecular ions that reflect the real chemical components and structures of the samples, allowing molecular analysis (e.g., molecular imaging) using ToF-SIMS. Therefore, it is very important to distinguish which ion signals may come from damage-recombination processes. The interesting ions in this research are solvated Li^+ ions, solvated anions, and Li^+−anion clusters. Li^+, salt anions, and solvent molecules exist in the electrolytes before SIMS measurement, not arising from damage induced by ion bombardment. Therefore, it is reasonable to say the interesting ions in this research are most probably not (or to a very limited degree) interfered by damage-recombination processes.

Ionization Yields. In SIMS analysis, it is well-known that quantification analysis is normally challenging because different species may have different ionization yields. In this research, this issue may not affect our conclusions because most interesting ions are either Li^+-attached positive ions or anion-attached negative ions. It has been reported that Cs^+-attached

DOI: 10.1021/acs.analchem.7b04921
Anal. Chem. 2018, 90, 3341−3348

positive ions can be used for quantification of different chemical species in depth profiling using Cs^+ sputtering, indicating Cs^+-attached positive ions may have similar ionization yields.[55−57] If so, it is reasonable to expect that Li^+-attached positive ions have similar ionization yields, too, because both Cs and Li are alkali metals, and they share similar chemical properties. Moreover, we have examined K^+- and H^+-attached water cluster ions using a KOH aqueous solution. The data (Figures S-7, S-8, and S-9) show a slow change of $[K + (H_2O)_n]^+$ and $[H + (H_2O)_n]^+$ signal intensities with increasing of solvated water molecule numbers, supporting that not only $[K + (H_2O)_n]^+$ or $[H + (H_2O)_n]^+$ ions may have similar ionization yields, but also all $[K + (H_2O)_n]^+$ and $[H + (H_2O)_n]^+$ ions are reasonably stable in vacuum. Besides, it is intriguing that there existed intensity anomaly at $[H + (H_2O)_{21}]^+$ and a distinct intensity drop between $[H + (H_2O)_{21}]^+$ and $[H + (H_2O)_{22}]^+$ in the spectrum (Figure S-9), suggesting the special stability of the magic number ion $[H + (H_2O)_{21}]^+$, which is similar to the results obtained by other different types of experiments.[58−61] Based on this, we are reasonably sure that the sharp ion intensity difference discussed in this work, such as that between $[Li + (EC)_3]^+$ and $[Li + (EC)_4]^+$ (Figure S-4), can be mainly attributed to difference in the stability of those ions.

CONCLUSIONS

In this work, in situ liquid SIMS was used to examine ion−solvent molecular interactions in three electrolyte compositions. Very solid molecular evidence supports that Li^+ is preferentially solvated with EC in $LiPF_6$ in EC−DMC, in excellent agreement with previous ESI-MS and NMR results. The preference for EC is, however, larger than observed in IR, Raman, and condensed phase BOMD simulations due to condensed phase effects arising from the second Li^+ solvation shell and beyond.[16]

More interestingly, solvation of PF_6^- was detected, indicating that anions solvation, though weak, is still not negligible. At the same time, preferential solvation of anions also exists. In addition, our data suggest that although the coordination number of a Li^+ ion can be as high as six, the first three combinations may be more stable than the others. Besides, in situ liquid SIMS can be used to examine formation of ion clusters in the electrolytes. Combined with computational techniques, in situ liquid SIMS serves as a powerful and sensitive experimental tool to elucidate the ion−solvent interactions in nonaqueous electrolytes for Li ion batteries.

ASSOCIATED CONTENT

Supporting Information

The Supporting Information is available free of charge on the ACS Publications website at DOI: 10.1021/acs.analchem.7b04921.

Set of negative ion spectra of 1.0 M $LiPF_6$ in EC−DMC electrolyte showing good data repeatability, solvation situation of all 64 Li^+ ions extracted from the MD simulation snapshot of the 1.0 M LiFSI in DME electrolyte, statistic comparison of signal intensities of interesting ions detected in 1.0 M $LiPF_6$ in EC−DMC electrolyte in both positive and negative ion modes, an in situ liquid SIMS spectrum of a 0.1 M KOH aqueous solution in the positive ion mode, the signal intensity trends of $[K + (H_2O)_n]^+$, $[H + (H_2O)_n]^+$ cluster ions in the positive ion spectrum of a 0.1 M KOH aqueous solution, and for readers' convenience also SIMS spectra of three solvents, including EC−DMC (1:2 v:v), DMC, and DME in both positive and negative ion modes (PDF)

AUTHOR INFORMATION

Corresponding Authors

*E-mail: zihua.zhu@pnnl.gov. Tel.: +1-509-371-6240 (Z.Z.).
*E-mail: fuyi.wang@iccas.ac.cn. Tel.: +86-10-62529069 (F.W.).
*E-mail: zhijie.xu@pnnl.gov. Tel.: +1-509-372-4885 (Z.X.).

ORCID

Yanyan Zhang: 0000-0002-2048-145X
Wu Xu: 0000-0002-2685-8684
Chongmin Wang: 0000-0003-3327-0958
Donald R. Baer: 0000-0003-0875-5961
Oleg Borodin: 0000-0002-9428-5291
Kang Xu: 0000-0002-6946-8635
Fuyi Wang: 0000-0003-0962-1260
Zihua Zhu: 0000-0001-5770-8462

Notes

The authors declare no competing financial interest.

ACKNOWLEDGMENTS

This work was supported by an FY2016 open call LDRD fund of the Pacific Northwest National Laboratory (PNNL). A U.S. patent (15/240,937) based on the electrochemical cell for Li ion battery research was filed on 08/18/2016. The work was performed at EMSL, a national scientific user facility sponsored by the Department of Energy's Office of Biological and Environmental Research located at PNNL. The authors thank Dr. Kazuhiko Murata of Nippon Shokubai Co., Ltd. for supplying the LiFSI salt without charge. F.W. and Y.Z. thank the NSFC (Grant Nos. 21127901, 21575145, 21621062) for support.

REFERENCES

(1) Xu, K. *Chem. Rev.* **2014**, *114*, 11503−11618.
(2) Xu, K. *J. Electrochem. Soc.* **2007**, *154*, A162−A167.
(3) Bogle, X.; Vazquez, R.; Greenbaum, S.; Cresce, A. v. W.; Xu, K. *J. Phys. Chem. Lett.* **2013**, *4*, 1664−1668.
(4) Winter, M. *Z. Phys. Chem.* **2009**, *223*, 1395.
(5) Xu, K. *Chem. Rev.* **2004**, *104*, 4303−4418.
(6) Burba, C. M.; Frech, R. *J. Phys. Chem. B* **2005**, *109*, 15161−15164.
(7) Chapman, N.; Borodin, O.; Yoon, T.; Nguyen, C. C.; Lucht, B. L. *J. Phys. Chem. C* **2017**, *121*, 2135−2148.
(8) Seo, D. M.; Reininger, S.; Kutcher, M.; Redmond, K.; Euler, W. B.; Lucht, B. L. *J. Phys. Chem. C* **2015**, *119*, 14038−14046.
(9) Yang, L.; Xiao, A.; Lucht, B. L. *J. Mol. Liq.* **2010**, *154*, 131−133.
(10) Reddy, V. P.; Smart, M. C.; Chin, K. B.; Ratnakumar, B. V.; Surampudi, S.; Hu, J.; Yan, P.; Surya Prakash, G. K. *Electrochem. Solid-State Lett.* **2005**, *8*, A294−A298.
(11) Morita, M.; Asai, Y.; Yoshimoto, N.; Ishikawa, M. *J. Chem. Soc., Faraday Trans.* **1998**, *94*, 3451−3456.
(12) Giorgini, M. G.; Futamatagawa, K.; Torii, H.; Musso, M.; Cerini, S. *J. Phys. Chem. Lett.* **2015**, *6*, 3296−3302.
(13) Allen, J. L.; Borodin, O.; Seo, D. M.; Henderson, W. A. *J. Power Sources* **2014**, *267*, 821−830.
(14) El Kazzi, M.; Czekaj, I.; Berg, E. J.; Novák, P.; Brown, M. A. *Top. Catal.* **2016**, *59*, 628−634.
(15) Cui, W.; Lansac, Y.; Lee, H.; Hong, S.-T.; Jang, Y. H. *Phys. Chem. Chem. Phys.* **2016**, *18*, 23607−23612.
(16) Borodin, O.; Olguin, M.; Ganesh, P.; Kent, P. R. C.; Allen, J. L.; Henderson, W. A. *Phys. Chem. Chem. Phys.* **2016**, *18*, 164−175.

DOI: 10.1021/acs.analchem.7b04921
Anal. Chem. 2018, 90, 3341−3348

(17) Ganesh, P.; Jiang, D.-e.; Kent, P. R. C. *J. Phys. Chem. B* **2011**, *115*, 3085−3090.
(18) Korsun, O. M.; Kalugin, O. N.; Fritsky, I. O.; Prezhdo, O. V. *J. Phys. Chem. C* **2016**, *120*, 16545−16552.
(19) Malliakas, C. D.; Leung, K.; Pupek, K. Z.; Shkrob, I. A.; Abraham, D. P. *Phys. Chem. Chem. Phys.* **2016**, *18*, 10846−10849.
(20) Ong, M. T.; Bhatia, H.; Gyulassy, A. G.; Draeger, E. W.; Pascucci, V.; Bremer, P. T.; Lordi, V.; Pask, J. E. *J. Phys. Chem. C* **2017**, *121*, 6589−6595.
(21) Kumar, N.; Seminario, J. M. *J. Phys. Chem. C* **2016**, *120*, 16322−16332.
(22) Borodin, O.; Smith, G. D. *J. Phys. Chem. B* **2009**, *113*, 1763−1776.
(23) Liu, B.; Xu, W.; Yan, P.; Sun, X.; Bowden, M. E.; Read, J.; Qian, J.; Mei, D.; Wang, C.-M.; Zhang, J.-G. *Adv. Funct. Mater.* **2016**, *26*, 605−613.
(24) Wan, C.; Hu, M. Y.; Borodin, O.; Qian, J.; Qin, Z.; Zhang, J.-G.; Hu, J. Z. *J. Power Sources* **2016**, *307*, 231−243.
(25) Qian, J.; Henderson, W. A.; Xu, W.; Bhattacharya, P.; Engelhard, M.; Borodin, O.; Zhang, J.-G. *Nat. Commun.* **2015**, *6*, 6362.
(26) Matsuda, Y.; Fukushima, T.; Hashimoto, H.; Arakawa, R. *J. Electrochem. Soc.* **2002**, *149*, A1045−A1048.
(27) von Cresce, A.; Xu, K. *Electrochem. Solid-State Lett.* **2011**, *14*, A154−A156.
(28) von Wald Cresce, A.; Borodin, O.; Xu, K. *J. Phys. Chem. C* **2012**, *116*, 26111−26117.
(29) Xiang, H.; Mei, D.; Yan, P.; Bhattacharya, P.; Burton, S. D.; von Wald Cresce, A.; Cao, R.; Engelhard, M. H.; Bowden, M. E.; Zhu, Z.; Polzin, B. J.; Wang, C.-M.; Xu, K.; Zhang, J.-G.; Xu, W. *ACS Appl. Mater. Interfaces* **2015**, *7*, 20687−20695.
(30) von Wald Cresce, A.; Gobet, M.; Borodin, O.; Peng, J.; Russell, S. M.; Wikner, E.; Fu, A.; Hu, L.; Lee, H.-S.; Zhang, Z.; Yang, X.-Q.; Greenbaum, S.; Amine, K.; Xu, K. *J. Phys. Chem. C* **2015**, *119*, 27255−27264.
(31) Zheng, D.; Qu, D.; Yang, X.-Q.; Lee, H.-S.; Qu, D. *ACS Appl. Mater. Interfaces* **2015**, *7*, 19923−19929.
(32) Cresce, A. V.; Russell, S. M.; Borodin, O.; Allen, J. A.; Schroeder, M. A.; Dai, M.; Peng, J.; Gobet, M. P.; Greenbaum, S. G.; Rogers, R. E.; Xu, K. *Phys. Chem. Chem. Phys.* **2017**, *19*, 574−586.
(33) Suo, L.; Hu, Y.-S.; Li, H.; Armand, M.; Chen, L. *Nat. Commun.* **2013**, *4*, 1481.
(34) Suo, L.; Borodin, O.; Gao, T.; Olguin, M.; Ho, J.; Fan, X.; Luo, C.; Wang, C.; Xu, K. *Science* **2015**, *350*, 938−943.
(35) Yang, L.; Yu, X.-Y.; Zhu, Z.; Iedema, M. J.; Cowin, J. P. *Lab Chip* **2011**, *11*, 2481−2484.
(36) Zhu, Z.; Zhou, Y.; Yan, P.; Vemuri, R. S.; Xu, W.; Zhao, R.; Wang, X.; Thevuthasan, S.; Baer, D. R.; Wang, C.-M. *Nano Lett.* **2015**, *15*, 6170−6176.
(37) Ding, Y.; Zhou, Y.; Yao, J.; Szymanski, C.; Fredrickson, J.; Shi, L.; Cao, B.; Zhu, Z.; Yu, X.-Y. *Anal. Chem.* **2016**, *88*, 11244−11252.
(38) Yu, J.; Zhou, Y.; Hua, X.; Liu, S.; Zhu, Z.; Yu, X.-Y. *Chem. Commun.* **2016**, *52*, 10952−10955.
(39) Wang, Z.; Zhang, Y.; Liu, B.; Wu, K.; Thevuthasan, S.; Baer, D. R.; Zhu, Z.; Yu, X.-Y.; Wang, F. *Anal. Chem.* **2017**, *89*, 960−965.
(40) Zhou, Y.; Yao, J.; Ding, Y.; Yu, J.; Hua, X.; Evans, J. E.; Yu, X.; Lao, D. B.; Heldebrant, D. J.; Nune, S. K.; Cao, B.; Bowden, M. E.; Yu, X.-Y.; Wang, X.-L.; Zhu, Z. *J. Am. Soc. Mass Spectrom.* **2016**, *27*, 2006−2013.
(41) Borodin, O. *J. Phys. Chem. B* **2009**, *113*, 11463−11478.
(42) Yang, L.; Zhu, Z.; Yu, X.-Y.; Thevuthasan, S.; Cowin, J. P. *Anal. Methods* **2013**, *5*, 2515−2522.
(43) Borodin, O.; Olguin, M.; Spear, C. E.; Leiter, K.; Knap, J. *Nanotechnology* **2015**, *26*, 354003.
(44) Ding, F.; Xu, W.; Graff, G. L.; Zhang, J.; Sushko, M. L.; Chen, X.; Shao, Y.; Engelhard, M. H.; Nie, Z.; Xiao, J.; Liu, X.; Sushko, P. V.; Liu, J.; Zhang, J.-G. *J. Am. Chem. Soc.* **2013**, *135*, 4450−4456.
(45) Zheng, J.; Engelhard, M. H.; Mei, D.; Jiao, S.; Polzin, B. J.; Zhang, J.-G.; Xu, W. *Nature Energy* **2017**, *2*, 17012.
(46) Wang, Y. X.; Balbuena, P. B. *Int. J. Quantum Chem.* **2005**, *102*, 724−733.
(47) Postupna, O. O.; Kolesnik, Y. V.; Kalugin, O. N.; Prezhdo, O. V. *J. Phys. Chem. B* **2011**, *115*, 14563−14571.
(48) Smith, J. W.; Lam, R. K.; Sheardy, A. T.; Shih, O.; Rizzuto, A. M.; Borodin, O.; Harris, S. J.; Prendergast, D.; Saykally, R. J. *Phys. Chem. Chem. Phys.* **2014**, *16*, 23568−23575.
(49) Honda, F.; Lancaster, G. M.; Fukuda, Y.; Rabalais, J. W. *J. Chem. Phys.* **1978**, *69*, 4931−4937.
(50) Garrison, B. J.; Winograd, N.; Harrison, D. E. *J. Chem. Phys.* **1978**, *69*, 1440−1444.
(51) Zhou, H.; Chan, C.-M.; Weng, L.-T.; Ng, K.-M.; Li, L. *Surf. Interface Anal.* **2002**, *33*, 932−939.
(52) Kanski, M.; Garrison, B. J.; Postawa, Z. *J. Phys. Chem. Lett.* **2016**, *7*, 1559−1562.
(53) Moss, F. R.; Boxer, S. G. *J. Am. Chem. Soc.* **2016**, *138*, 16737−16744.
(54) Yu, X.; Yu, J.; Zhou, Y.; Zhang, Y.; Wang, J.; Evans, J. E.; Yu, X.-Y.; Wang, X.-L.; Zhu, Z. *Rapid Commun. Mass Spectrom.* **2017**, *31*, 2035−2042.
(55) Magee, C. W.; Harrington, W. L.; Botnick, E. M. *Int. J. Mass Spectrom. Ion Processes* **1990**, *103*, 45−56.
(56) Gnaser, H. *J. Vac. Sci. Technol., A* **1994**, *12*, 452−456.
(57) Niehuis, E.; Grehl, T.; Kollmer, F.; Moellers, R.; Rading, D.; Kersting, R.; Hagenhoff, B. *Surf. Interface Anal.* **2011**, *43*, 204−206.
(58) Nagashima, U.; Shinohara, H.; Nishi, N.; Tanaka, H. *J. Chem. Phys.* **1986**, *84*, 209−214.
(59) Hulthe, G.; Stenhagen, G.; Wennerström, O.; Ottosson, C.-H. *J. Chromatogr. A* **1997**, *777*, 155−165.
(60) Hermann, V.; Kay, B. D.; Castleman, A. W. *Chem. Phys.* **1982**, *72*, 185−200.
(61) Lancaster, G. M.; Honda, F.; Fukuda, Y.; Rabalais, J. W. *J. Am. Chem. Soc.* **1979**, *101*, 1951−1958.

DOI: 10.1021/acs.analchem.7b04921
Anal. Chem. 2018, 90, 3341−3348